Graduate Student Recruitment and Training Support

Report for

One Ajahn, One Project

May 2003 through April 2004

Academic Year 2546

Associate Professor Dr. Kenneth J. Haller
School of Chemistry
Institute of Science
Suranaree University of Technology
Nakhon Ratchasima 30000

HYDROTHERMAL SYNTHESIS AND CHARACTERIZATION OF $NH_3CH_2CH_2CH_2NH_3^{2+}$ $[(VO)_2(VO_4)_2]^{2-}$

Samroeng Krachodnok, Kittipong Chainok and Kenneth J. Haller

School of Chemistry, Institute of Science, Suranaree University of Technology, Nakhon Ratchasima 3000, Thailand

Introduction

In the past decade design and synthesis of organic-inorganic hybrid materials has received considerable attention, not only to the variety of structural types and bonding geometries but also due to potential applications in fields such as catalysis [1], electronic conductivity [2], magnetism [3], medicine [4] and others. One of the most powerful methods for the preparation of these hybrid materials and other important solids is the hydrothermal synthesis technique. The hydrothermal method is particularly suitable for fabrication of organic-inorganic hybrid metal oxide materials since the traditional methods of synthesizing the metal oxide frameworks rely on high temperatures which would destroy the organic template molecules. Organic amines have been used extensively as templates for preparation of many of these hybrid materials under hydrothermal conditions. The organic amine is generally both a charge-compensating cation and a space-filling moiety, and may also function as a ligand to the metal.

Experimental

The synthesis of $NH_3CH_2CH_2CH_2NH_3^{2+}[(VO)_2(VO_4)_2]^{2-}$ was carried out under hydrothermal conditions: a mixture of V_2O_5 (0.5002 g), $CoCl_2{\cdot}6H_2O$ (0.6541 g), 1,3-DAP (0.4097 g), HCl (0.1003 g), and H_2O (29.4 g) in a molar ratio of 1:1:2:1:593 was stirred for 30 min in air, the solution/mixture was transferred and sealed in a 125 mL teflon-lined stainless steel autoclave (Parr bomb), and heated to 180 °C under autogenous pressure for 4 days before cooling to room temperature. The acidity of the medium was at constant pH of ~7-8 before and after the reaction. Brown-black crystals were filtered off, washed with water, and air-dried at room temperature. The compound is insoluble in water and common organic solvents.

The morphology of the crystalline product (Figure 1) was observed by a scanning electron microscope (Jeol model JSM-6400 SEM) equipped with an energy dispersive x-ray fluorescence microanalyzer (WDX-100 EDX attachment). The IR spectrum was recorded in the range 400-4000 cm^{-1} on a Perkin-Elmer model Spectrum GX FTIR spectrometer using a KBr pellet. TG analysis was carried out on a Perkin-Elmer TGA7 Thermal Analyzer in flowing N_2 with a heating rate of 10 °C min^{-1}. X-ray crystallographic data were collected from a hexagonal crystal with a Bruker-Nonius KappaCCD four-circle diffractometer equipped with a graphite monochromator and 0.5 mm *ifg* capilliary collimator.

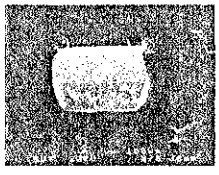

Figure 1. SEM picture of one crystal of $(1,3\text{-}H_2DAP)[(VO)_2(VO_4)_2]$

Crystal Data: $(V_2O_8)(C_5H_{12}N_2)$; M_r = 439.90 Daltons; monoclinic, $P2_1/n$ (No. 14); a = 7.975(3), b = 9.986(2), c = 15.629(3) Å, β = 100.66(3), V = 1223.4(5) Å^3; T = 298 K; Z = 4; d_{calc} = 2.39 Mg/m^3; μ = 30.1 cm^{-1}; *MoKα*, λ = 0.71073 Å; $2\theta_{max}$ = 55°; 16,076 data; 2778 unique data. R_{merg} = 0.079. Final model: anisotropic nonhydrogen atoms, idealized riding hydrogen atoms; final R_1 = 0.038 for 2407 data with $I(h) > 3\sigma(I(h))$ from SHELXTL [5].

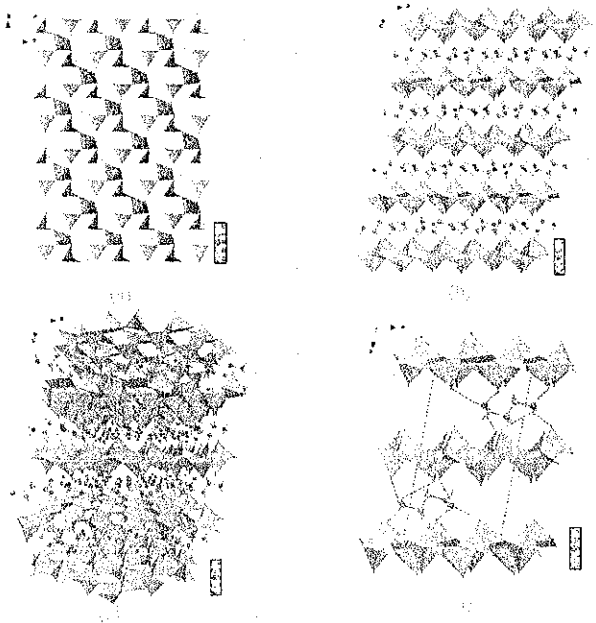

Figure 2. (a) Projection drawing oriented perpendicular to the 2D polyhedral network. (b) Projection drawing oriented parallel to the 2D polyhedral network showing the alternating inorganic vanadium oxide and organic layers. (c) Perspective drawing as in b. (d) The hydrogen bonding between H_2DAP and the vanadium oxide layers.

Results, Discussion, and Conclusions

The EDX spectrum indicates the presence of both vanadium (96%) and cobalt (4%). There is no evidence for cobalt in the structure from the crystal studied, and all the crystals examined can be related to the same morphology as the data crystal. It is possible that there is a minor solid state product that either deposits on the surface of the crystals or forms as an invisible noncrystalline deposit along with the crystals.

The crystal structure consists of two dimensional anionic vanadium oxide networks separated by organic layers of $1,3\text{-}H_2DAP$ cations as illustrated in Figure 2(b). The vanadium oxide layers are constructed from equal numbers of VO_4 tetrahedrons each containing one vanadyl oxygen atom, and VO_5 square pyramids with vanadyl oxygen atoms in the apical positions. The square pyramids occur in basal edge-sharing pairs with the vanadyl groups projecting to opposite sides of the combined basal planes. Each oxygen atom shared between the two square pyramids is also shared with one VO_4 tetrahedra (μ_3-O). The remaining four oxygen atoms of the basal planes are also shared with VO_4 tetrahedra (μ_2-O). The resulting network is illustrated as a polyhedral representation in Figure 2(a). It can be seen that the non-bridging apical positions (the vanadyl groups) of both the tetrahedra and the square pyramids alternate above and below the plane as one moves across the layer.

The vanadyl groups are good hydrogen bond acceptors, so it is not surprising to find that all six hydrogen bond donors form hydrogen bonds with the vanadyl groups as illustrated in Figure 2(d). Three of the hydrogen bonds involve two vanadyl groups (bifurcated hydrogen bonds) and three involve single vanadyl groups.

The IR spectrum is shown in Figure 3. The strong bands at 971 cm^{-1} are assigned to the terminal V=O stretching mode and the bands at 830, 631 and 560 cm^{-1} are consistent with symmetrical and asymmetrical M–O–M stretching modes. Bands at 1599, 1488 and 1187 cm^{-1} are characteristic of 1,3-DAP, and the bands in the 3009 and 3450 cm^{-1} regions can be attributed to N–H stretching.

The TG curve is shown in Figure 4. It can be divided into two stages. In the first stage from 270 to 370 °C, a 39% weight loss occurs, corresponding to the release of 1,3-DAP. A second stage in the temperature range of 630-780 °C shows a gradual weight gain of 2.8%, consistent with oxidation of the framework from V^{4+} to V^{5+}.

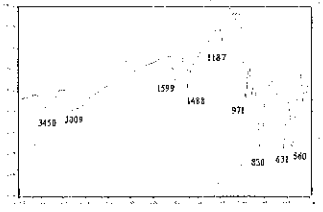

Figure 3. IR spectrum

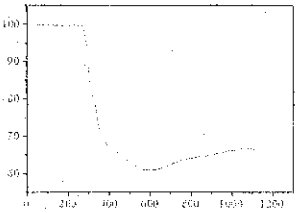

Figure 4. TGA spectrum

References

1. Botella, P.; López Nieto J. M.; Solsona, B.; Mifsud, A.; Márquez, F. (2002). *J. Catal.*, 209, 445-455.

2. Yang, S.; Song, Y.; Ngala, K.; Zavalij, P. Y.; Whittingham, M. (2003). *J. Power Sources*, 119-121, 239-246.

3. Alda, E.; Bazán, B.; Mesa, J. L.; Pizarro, J. L.; Arriortua, M. I.; Rojo, T. (2003). *J. Solid State Chem.*, 173, 101-108.

4. Saha, D. K.; Padhyde, S.; Anson, C. E.; Powell, A. K. (2002). *Inorg. Chem. Commun.*, 5, 1020-1027.

5. Sheldrick, G. M. (1997). SHELXTL Reference Manual, ver. 5.1, Bruker AXS, Inc., Madison.

Acknowledgements

We wish to thank Suranaree University of Technology for partial support of this research (grant SUT1-102-41-36-07), and for travel support to attend this meeting.